International Journal of Mass Spectrometry 195/196 (2000) 507–516

Low energy (0–14 eV) electron impact to CHF_2Cl at different phase conditions: medium enhanced desorption of anions

Frank Brüning, Petra Tegeder, Judith Langer, Eugen Illenberger*

Institut für Chemie–Physikalische und Theoretische Chemie, Freie Universität Berlin, Takustrasse 3, D-14195 Berlin, Germany

Received 16 June 1999; accepted 9 August 1999

Abstract

The formation of negative ions following low energy (0–14 eV) electron impact to CHF_2Cl under different phase conditions is studied including isolated gas phase molecules, free homogeneous clusters, and multilayer CHF_2Cl films condensed on a metallic substrate at cryogenic temperature. In the gas phase we observe three very weak resonances on the Cl^-, F^-, and H^- dissociative attachment (DA) channels peaking near 1.1, 3.4, and ≈6 eV, respectively. From clusters, we find solvated fragment ions of the form $Cl^- \cdot (CHF_2Cl)_n$ and $F^- \cdot (CHF_2Cl)_n$ but no parent anions or undissociated larger cluster ions. Electron impact to condensed CHF_2Cl leads to remarkably strong resonance features in the desorption yield with peak maxima at 9.7 (Cl^-, F^-) and 5.5 eV (H^-). The absolute cross section for ion desorption is about 2 orders of magnitude higher than the gas phase DA cross section. This observation is explained in terms of a particular medium enhanced DA reaction at the surface based on the conversion of a short lived open channel resonance into a longer lived (closed channel) *Feshbach* resonance. (Int J Mass Spectrom 195/196 (2000) 507–516) © 2000 Elsevier Science B.V.

Keywords: Negative ions; Dissociative attachment; Desorption

---

1. Introduction

Halogenated methanes can effectively generate halogen ions via dissociative electron attachment (DA) [1–3], viz.

$$e^-(\varepsilon) + \mathrm{M} \rightarrow \mathrm{M}^{-(*)} \rightarrow \mathrm{R} + \mathrm{X}^- \tag{1}$$

where at a particular resonance energy (ε) a transient negative ion $M^{-(*)}$ (TNI) is formed by electron capture which decomposes into a neutral radical and a halogen ion.

In this article we present a comparative study on negative ion formation from gas phase and condensed phase CHF_2Cl following low energy (0–14 eV) electron impact. By gas phase we refer to both single molecules in an effusive molecular beam and homogeneous clusters formed by supersonic beam expansion and by condensed phase to negative ion desorption from CHF_2Cl molecules deposited in multilayer amounts under UHV conditions on a cold (30 K) substrate.

The DA cross section for gas phase chlorofluoromethanes can vary within many orders of magnitude dependent on the composition of the particular

---

* Corresponding author. E-mail: iln@chemie.fu-berlin.de

Dedicated to Bob Squires for his many seminal contributions to mass spectrometry and ion chemistry.

PII S1387-3806(99)00171-2

molecule [4–6]. Generally one finds that (1) in compounds containing both F and Cl atoms the Cl^- channel always dominates over F^-, (2) F^- appears at considerable higher energies than Cl^-, and (3) the DA cross section strongly increases with the number of chlorine atoms in the compound, much more than expected from any steric effect. This behaviour is related to the underlying thermodynamic parameters and the mechanism of the overall process including the difference in the strengths between the C–F and the C–Cl bond, the energy level of the associated precursor ion and the effect of electron loss (autodetachment) in the decay of the TNI (see below). Rule (2) is already obvious from thermodynamics: since the C–F bond dissociation energy exceeds the electron affinity of F (3.4 eV) by 1 to 2 eV [7] the F^- channel is always endothermic by that amount. The C–Cl bond dissociation energy, on the other hand, is comparable or lower than the electron affinity of Cl (3.62 eV) [7], which makes the Cl^- DA channel approximately thermoneutral or even exothermic. However, apart from thermodynamics, the usual observation is that DA resonances decomposing into F^- are located considerably above the exit channel whereas Cl^- appears near the thermodynamic threshold. This is related to the electronic structure of the corresponding precursor ion. For a TNI predominantly dissociating into F^-, the involved molecular orbital (MO) is expected to possess appreciable σ*(C–F) character. These antibonding MOs are usually more repulsive in the Franck-Condon area governing the initial transition than their σ*(C–Cl) counterparts and thus considerably above the energy of the DA limit. In CF_4, e.g. the DA process (F^- formation) is endothermic by 2 eV whereas the maximum of the involved TNI (DA resonance) is at 6.8 eV and thus nearly 4 eV above the energetic threshold. The DA cross section (peak value) is 1.6×10^{-18} cm^2 [8,9]. In contrast, the DA reaction in CCl_4 (Cl^- formation) is exothermic by 0.6 eV and the cross section for Cl^- exceeds 10^{-14} cm^2 below 100 meV [1,10,11]. Cross section changes with the number of halogen atoms can be seen most dramatically in the case of the chloromethanes. According to recent experimental and theoretical studies [12,13] the DA cross section in methylchloride (resonance energy located at 2.2 eV) is below 10^{-23} cm^2 at room temperature, which is nearly 10 orders of magnitude (!) below that in CCl_4 (supra vide). The obvious implication for any mass spectrometric study is then the inherent problem of (very) small impurities of a compound having a high DA cross section in a sample possessing a low cross section.

The physical basis of such large cross section differences essentially relies on two phenomena relevant in DA involving both the formation and dissociation of the TNI. First, from basic principles (Wigner threshold laws [14] and scattering theory [15,16]) one expects the capture cross section to increase with decreasing electron energy ($\sigma \propto \varepsilon^{-1/2}$ at threshold and $\sigma \propto \varepsilon^{-1}$ at higher energy) and second, once the TNI is formed, fragmentation into the radical and anion can be considerably suppressed in favour of the competitive process of electron loss (autodetachment) recovering the neutral system

$$M^{-(*)} \rightarrow M^{(*)} + e^- \tag{1a}$$

This competitive channel is considered to become more dominant with increasing electron energy. Thus, both phenomena contribute in the same way to the energy dependence of the DA reaction. The large cross section difference previously illustrated cannot solely be explained by the reciprocal energy dependence of the capture cross section including steric effects; it is, rather, due to a dramatic decrease of the survival probability of the TNI with energy, i.e. the probability that the additional electron is kept by the system during dissociation. In terms of potential energy curves (Fig. 1) autodetachment can occur up to the point, where the anionic curve crosses that of the neutral system. CCl_4^- is formed near 0 eV (the anionic curve crosses the potential energy curve of a neutral molecule near the minimum) and hence has a probability close to unity to survive dissociation into $Cl^- + CCl_3$ without electron loss. CH_3Cl^-, on the other hand, is formed at a higher energy where the exceedingly dominant decay channel is autodetachment (1a).

Electron attachment to gas phase molecules usually leads to prompt fragmentation (DA) and only for larger compounds (SF_6, C_{60}, etc. [17]) the undissoci-

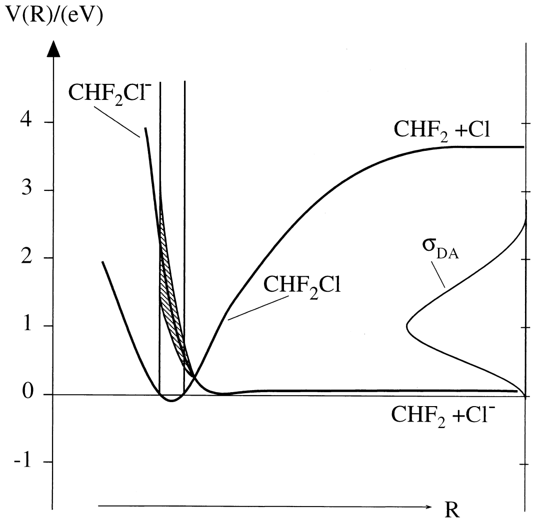

Fig. 1. Diatomic-like potential energy curve illustrating DA via ground state CHF_2Cl^-. The width of the anionic potential energy curve is due to the lifetime of the TNI with respect to electron loss (autodetachment width).

ated parent anion can be observed on the mass spectrometric time scale. In clusters, on the other hand, collision partners are easily available to remove the excess energy generating the relaxed parent anion (provided the molecule possesses a positive electron affinity) or larger undissociated cluster ions. Electron attachment to clusters has in fact been shown to be a very effective method to generate parent anions in the gas phase [17,18].

In the condensed phase the situation for a DA reaction is appreciably modified [17,19] as now effective pathways for energy dissipation become operative and, further, the reaction products may either remain adsorbed at the surface or be emitted into vacuum. From these modifications alone one would rather expect a decrease of the reactivity (cleavage of a chemical bond) in the course of electron capture. Coupling to environmental molecules, however, can also modify the lifetime of the TNI with respect to autodetachment [channel (1a)], which can lead to an increase of the reaction cross section.

From these brief general considerations we expect a rather low DA cross section for the present compound CHF_2Cl [rule (3)]. As we shall demonstrate in the following this is in fact the case for the gas phase species. From condensed CHF_2Cl, on the other hand, we observe very effective desorption of Cl^- and F^- and also of H^- with the latter ion barely observable from gas phase CHF_2Cl.

2. Experimental

A detailed description of the experimental arrangements for the gas phase and the condensed phase studies can be found in a recent review from our laboratory [17]. Both the gas phase and condensed phase arrangement is equipped with a trochoidal electron monochromator (TEM [20]) delivering a beam of energy selected electrons (0.1–0.2 eV FWHM) of sufficient intensity (20–50 nA) down to very low energies. This is achieved by a weak homogeneous magnetic field which aligns the low energy electrons and also performs energy selection of the electrons in a crossed electrostatic/magnetic field configuration representing the heart of the TEM. Experiments on single gas phase molecules are performed by crossing the electron beam with an effusive molecular beam from a capillary directly fitted to the reaction chamber. The neutral cluster beam is generated by supersonic expansion of CHF_2Cl seeded in Ar (1:10) through an 80 μm nozzle.

In the desorption experiment a volumetrically determined amount of CHF_2Cl is condensed on a monocrystalline Au substrate held at cryogenic temperature (30 K) by means of a closed cycle He refrigerator. To avoid surface contamination or charging of the film, the desorption spectra presented here refer to the first scan on a newly deposited film after evaporation of the previous one by heating the substrate. The base pressure in the UHV system is in the 10^{-10} mbar range.

In each case negative ions created by the interaction of the electron beam with the target (effusive molecular beam, supersonic beam, or molecular film) are extracted from the interaction region by a weak homogeneous electric field and recorded by a quadrupole mass spectrometer as a function of the primary electron energy.

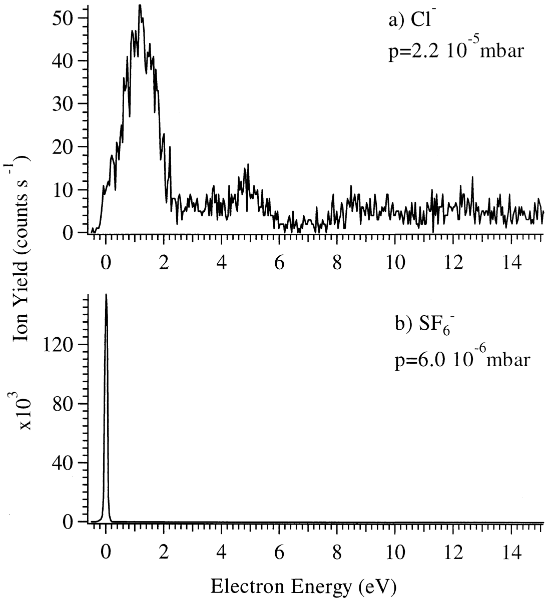

Fig. 2. Formation of Cl^- from gas phase CHF_2Cl in the effusive molecular beam and SF_6^- calibration peak recorded at the indicated pressure (ionization gauge reading, see the text).

The calibration of the electron energy scale in the gas phase experiments is performed by recording the well known “0 eV” SF_6^- resonance. In the condensed phase we use the onset of the electron injection curve (which is always monitored in the course of a desorption scan) as 0 eV for the vacuum level [17].

3. Results and discussion

Figs. 2 and 3 present the energy dependence of the relative cross sections for the fragment ions Cl^-, F^-, and H^- observed from gas phase CHF_2Cl plotted in absolute count rates. The indicated pressure refers to the reading at the ionization gauge; the actual pressure in the interaction volume is about 3 orders of magnitude higher [25]. Included in Fig. 2 is the SF_6^- calibration peak. As an example for the results obtained from clusters Fig. 4 shows the naked fragment ion F^- and the solvated fragment ions $F^- \cdot (CHF_2Cl)_1$ and $F^- \cdot (CHF_2Cl)_2$ arising from electron attachment to clusters at a stagnation pressure of 1 bar. Fig. 5 finally shows the desorption spectra obtained from a two layer CHF_2Cl film directly deposited on the metal substrate. From these results it can be seen that both the ion production from the gas phase (isolated molecules and clusters) and the desorption of ions from condensed CHF_2Cl show pronounced resonance profiles, however at very different energies.

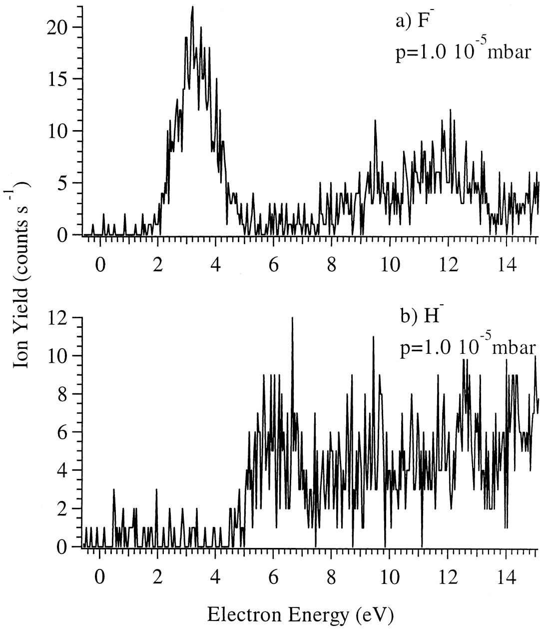

Fig. 3. Formation of F^- and H^- from gas phase CHF_2Cl in the effusive beam.

Before we discuss the cross section and mechanism of DA to gas phase CHF_2Cl and desorption from condensed phase we shall briefly consider the energetics of the corresponding reaction channels. In the gas phase the lowest DA channels for the three observed fragments are

$$e^- + CHF_2Cl \rightarrow CHF_2 + Cl^- \quad (\Delta H_0 = 0.14 \pm 0.1\ \mathrm{eV}) \qquad (2a)$$

$$e^- + CHF_2Cl \rightarrow CHFCl + F^- \quad (\Delta H_0 = 1.76 \pm 0.2\ \mathrm{eV}) \qquad (2b)$$

$$e^- + CHF_2Cl \rightarrow CF_2Cl + H^- \quad (\Delta H_0 = 3.6 \pm 0.1\ \mathrm{eV}) \qquad (2c)$$

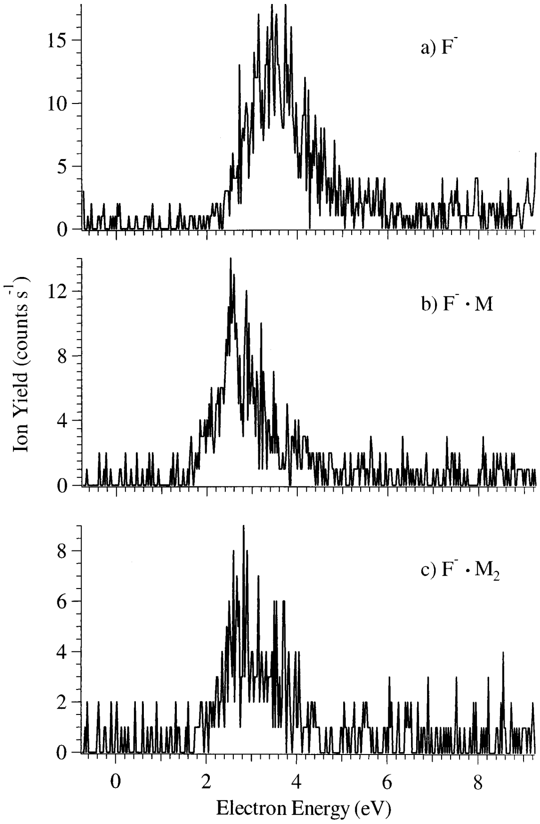

Fig. 4. Formation of the solvated ions $F^- \cdot (CHF_2Cl)_n$ ($n = 0$–2) from CHF_2Cl clusters in the supersonic beam recorded at a stagnation pressure of 1 bar.

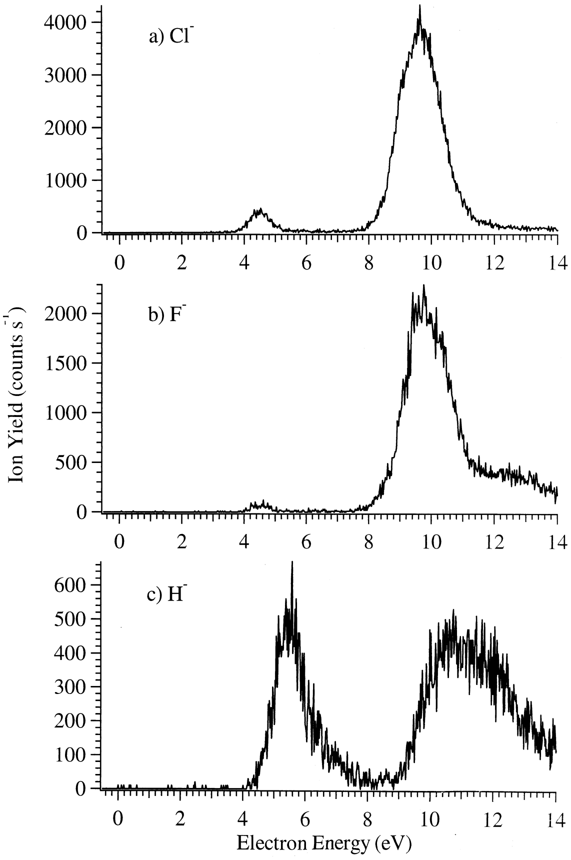

Fig. 5. Desorption of Cl^-, F^-, and H^- from a two layer CHF_2Cl directly deposited on the metallic substrate at 30 K.

with their thermodynamic thresholds (ΔH_0) calculated from the heat of formation for the parent molecule ΔH_f^o (CHF_2Cl) = −482.6 kJ mol^{-1} and those for the neutral fragments

ΔH_f^o (CHF_2) = −238.9 ± 4 kJ mol^{-1},
ΔH_f^o (CHFCl) = −60.7 ± 10 kJ mol^{-1},
ΔH_f^o (CF_2Cl) = −279.1 ± 8.3 kJ mol^{-1},
ΔH_f^o (Cl) = 121.3 kJ mol^{-1},
ΔH_f^o (F) = 79.4 ± 0.3 kJ mol^{-1}, and
ΔH_f^o (H) = 218 kJ mol^{-1},

and the electron affinities known with spectroscopic accuracy (only two digits are given here) [EA(Cl) = 3.62 eV, EA(F) = 3.40 eV, and EA(H) = 0.75 eV (all data taken from [7]). From these numbers, the corresponding bond dissociation energies are calculated as D(C–Cl) = 3.78 ± 0.1 eV, D(C–F) = 5.20 ± 0.1 eV, and D(C–H) = 4.37 ± 0.1 eV.

3.1. Isolated molecules

Concerning electron attachment to gas phase CHF_2Cl we find in the literature only two electron swarm studies yielding attachment rates of $k < 3.5 \times 10^{-13}$ cm^3 s^{-1} [21] and $k < 1.6 \times 10^{-13}$ cm^3 s^{-1} [22] for thermal electron energies. This corresponds to a thermal electron attachment cross section of $<3.5 \times 10^{-20}$ and $<1.6 \times 10^{-20}$ cm^2, respectively (for the underlying estimation see [17]). In swarm experiments the absolute value of the attachment rate is obtained from the loss of electrons in the pressence of an electron scavenger. Such a technique, however, does not directly account for the nature of the ions formed.

Returning to Fig. 2 it can be seen that the Cl^-

resonance peaks at 1.1 eV and that of F^- at 3.4 eV corresponding to an excess energy at the peak maximum of 1.0 eV (Cl^-) and 1.6 eV (F^-). The DA channel yielding Cl^- contains appreciable excess energy, though less than that of F^-. This is often the case if only one Cl atom is present in the molecule like in CF_3Cl [3,17] or CH_3Cl [12,13].

Fig. 1 also contains the SF_6^- calibration peak which we can use to obtain an estimation for the DA cross section at the resonance maximum. For SF_6 various independent swarm experiments [1,23] resulted in a thermal attachment rate near 2.5×10^{-7} cm^3 s^{-1} corresponding to a thermal attachment cross section of 2.5×10^{-14} cm^2. If we assume the same transmission and detection efficiency for SF_6^- and Cl^-, and take the absolute (pressure normalized) numbers from Fig. 2 we arrive at a peak value (at 1.1 eV) of $\approx 2 \times 10^{-18}$ cm^2 for the DA cross section yielding Cl^-. In actual practice one is faced with particular discrimination effects, which we shall not consider in detail, we only mention that the transmission of the quadrupole mass filter decreases appreciably towards higher masses. In addition, due to the reciprocal energy dependence of the attachment cross section, the count rate of the SF_6^- signal depends on the energy resolution and the ability, how far the energy of the electrons in the collision region can be pushed toward zero. The present value of $\approx 2 \times 10^{-18}$ cm^2 is thus only a crude estimation. With the absolute count rates from Figs. 2 and 3 we can further conclude that the DA cross section into F^- (at 3.4 eV) and H^- (near 6 eV) is in the order of $<10^{-18}$ cm^2. From Fig. 2 it can be seen that the cross section for thermal electrons (26 meV) is considerably lower than that at the Cl^- peak position and thus approaching the value derived from thermal swarm experiments (above).

In a recent nonthermal swarm study, Mayhew and co-workers [24] obtained one broad peak between 1.2 and 2.7 eV with the peak maximum at 2.0 eV and an attachment cross section of 4.8×10^{-19} cm^2 at the peak maximum. While the absolute cross section is at least in the same order of magnitude with that derived in the present study (via calibration on SF_6) there is an obvious discrepancy concerning the peak position. A comparison between both techniques, however is not straightforward as the swarm experiment is carried out in a buffer gas under atmospheric pressure. Further, the cross section is derived from the attachment rate by means of an unfolding technique which can also lead to artefacts.

In terms of MOs it is likely that the low energy Cl^- resonance (like in other fluorochlorocompounds) can be pictured as electron attachment yielding ground state CHF_2Cl^- which usually possesses pronounced antibonding σ^*(C–Cl) character. The low energy process can hence be described as direct dissociation into the two fragments $Cl^- + CHF_2$ along a repulsive potential energy surface (Fig. 1).

In spite of the expected direct dissociation, the Cl^- ion yield is exceptionally low, about 2 orders of magnitude lower than from the compound $CHFCl_2$, which was recently studied by our laboratory [25]. In this case the Cl^- DA cross section was located at 0.5 eV and the survival probability was estimated to be near 10%. In the CHF_2Cl the DA resonance is located at an appreciable higher energy (1.1 eV) and we can assume that the much lower DA cross section is essentially due to a lower survival probability of the TNI. This is indicated by the energy width of the anionic potential energy curve (Fig. 1), which is directly connected to the autodetachment lifetime.

3.2. Clusters

Electron attachment to clusters offers many possibilities to study the formation and evolution of NIRs at varying degree of aggregation [18]. Due to the “built in” three body collision it also presents a convenient way to generate the relaxed parent negative ions in the gas phase. In spite of a positive (adiabatic) electron affinity, single molecules usually undergo prompt DA. As shown in many studies, the undissociated parent anion (and larger undissociated cluster ions) can be detected following electron capture by the corresponding neutral clusters [18,26].

In CHF_2Cl, however, we neither find the monomeric anion (CHF_2Cl^-) nor larger undissociated cluster anions but only solvated fragment ions of the form $Cl^- \cdot (CHF_2Cl)_n$ and $F^- \cdot (CHF_2Cl)_n$. This indicates that the anionic potential energy surface has either only a very shallow minimum or is purely repulsive (Fig. 1).

Formation of the solvated ions $Cl^- \cdot (CHF_2Cl)_n$ and $F^- \cdot (CHF_2Cl)_n$ follows the usual trend [17]: they resemble the resonance profile of the corresponding gas phase DA process, however, subjected to a particular energy shift. This means that electron capture can be described on a molecular level, i.e. electron localization on an individual molecule, coupled to the neighbouring particles in the cluster. At larger stagnation pressure (formation of larger neutral clusters) one observes a slight red shift for a fixed product ion, whereas at fixed stagnation pressure some redshift in the resonance position is seen for the corresponding Cl^- solvated fragments (not shown here) with increasing size of the product ion. This general behaviour mirrors the increasing solvation energy with the size of the target cluster. One has to be aware, however, that the resonance position for a particular product ion is not the only result of the energy of the initial attachment event in the target cluster (i.e. the Franck-Condon transition creating a TNI in the target cluster and subjected to a particular solvation energy), it also contains the (energy dependent) decomposition dynamics generating the particular ion under observation. As an example, Fig. 4 shows the energy dependence of $F^- \cdot (CHF_2Cl)_n$ ($n = 0$–2) formation at a fixed stagnation pressure. While the naked fragment ion F^- can either result from a neutral monomer (scattered background molecule or monomer in the beam) or from a cluster of unknown size, the solvated fragment ions $F^- \cdot (CHF_2Cl)_n$ ($n = 1$–2) are necessarily products of a DA reaction to a cluster.

3.3. Desorption from condensed molecules

Fig. 5 presents the desorption spectra from a two multilayer CHF_2Cl film directly condensed onto the metallic substrate. The relative intensities and peak positions of these features are virtually independent on the thickness of the molecular film above completion of the second monolayer.

The peak positions in the resonant desorption profiles differ substantially from those obtained in gas phase DA. The most striking feature is that the low energy resonances appearing in the Cl^- (1.1 eV) and F^- (3.4 eV) fragments are almost completely suppressed in the desorption spectrum in favour of a strong resonance in the vicinity of 9.6 eV. At that energy, only a very weak intensity is seen from gas phase CHF_2Cl. On the other hand, the gas phase DA resonance yielding H^- ($\approx$6 eV) is not far from the prominent desorption feature ($\approx$5.5 eV). Interestingly, the relative intensity of desorbed fragment anions follows the same order as from gas phase DA, i.e. $Cl^- > F^- > H^-$. The usual situation within the halogens is that the light ion F^- is more intense than Cl^- in the desorption spectrum (see the following) [17]. This was also the observation in the recent study for the related compound $CHFCl_2$ [25].

By recording desorbed H^- one has to take care of possible contributions from H_2O which is an ubiquitous component at surfaces, also under UHV conditions. Electron impact around 8 eV leads to H^- desorption as previously shown by Sanche and coworkers [27]. To check possible contributions in the H^- signal from H_2O condensed from the background gas we monitored H^- desorption after exposition of the cold metallic substrate for 40 min to the background gas. This is a much longer period than the usual measuring cycle (deposition of the molecular film and taking a desorption scan) which is in the order of a few minutes. Such a procedure in fact results in some H^- intensity (100 counts s^{-1}) from a resonance feature in the 8–10 eV energy range, eventually due adsorbed background H_2O from the residual gas. The H^- feature in Fig. 5, however, is completely different which we thus ascribe to desorption from the CHF_2Cl film.

Since the ion desorption yields exhibit pronounced resonant structures it is likely that electron localization in condensed CHF_2Cl can still be described on a molecular site, i.e. formation of an individual TNI coupled to the medium. The energy of a negative ion located at a surface, however, will be modified by the environmental molecules. In a simplified scheme, this interaction can be divided into the (classical) attractive polarization interaction of the excess charge with the surrounding molecules and the (quantum mechanical) repulsive electronic exchange interaction (Pauli repulsion) [28–30]. The latter may only contribute to a significant degree if the extra electron resides in a spatially extended orbital.

If we assume the *net* interaction of the present TNI at the surface to be attractive by 1 eV (which is a reasonable number for halogencompounds as discussed in a number of previous investigations [31–33]) the initial transition will generate the TNI at the surface redshifted by this value with respect to the gas phase. The TNI then decomposes into a negatively charged and a neutral fragment (at the moment, we neglect multiple fragmentation). Desorption of the ionic fragment can occur if the kinetic energy released to the ion is sufficiently high, i.e. higher than its net attractive interaction with the environment. Apart from this energy constraint (kinetic energy filter in desorption) it is clear that desorption preferentially occurs for those orientations of the target compound with the C–X axis pointing away from the surface allowing direct X^- emission. For other orientations DA is still possible, however, postdissociation interactions of the fragment ion with the surrounding molecules will always be accompanied by some energy dissipation which will reduce the desorption probability. If we approximate the decomposition of the TNI at the surface as unimolecular and assume the same interaction energy (V_a) for the TNI and the fragment ion X^-, the energetic threshold for desorption becomes [17]

$$\varepsilon_d = (m_i/m)\, V_a + \Delta H_0 \tag{3}$$

with m_i and m representing the mass of the ionic and neutral fragments, respectively, and ΔH_0 the thermodynamic limit of the corresponding gas phase DA process. Note that in this context V_a is a positive number.

Expression (3) indicates that desorption of a heavy ionic fragment is energetically less favourable. This is simply a consequence of the principle of linear momentum conservation which results in more kinetic energy release to the light fragment ion. As mentioned above, one generally observes that desorption of F^- is more intense compared to Cl^-, which is apparently not the case in the present system. Such a behaviour can principally be explained by the following two effects: the unimolecular decomposition of the 9.7 eV resonance is more directional toward the Cl^- DA channel (releasing more kinetic energy) and/or the molecules at the surface of the molecular film have a preferential orientation for Cl^- desorption.

If we take the ΔH_0 numbers from above and assume $V_a = 1$ eV we expect the desorption threshold for Cl^- by 0.7 eV and that for F^- by 0.3 eV above the corresponding gas phase value (ΔH_0), i.e. $\varepsilon_d(Cl^-) \approx 0.8$ eV and $\varepsilon_d\,(F^-) \approx 2.0$ eV. For H^-, gas phase DA and desorption thresholds virtually coincide.

Returning to Fig. 5 we see that both the low energy Cl^- and F^- resonance are completely suppressed although the thermodynamic threshold is even below the energy of the corresponding gas phase DA maximum. Since the unimolecular decay of the TNI at the surface itself is subjected to a particular energy distribution, it is not surprising that the desorption probability is pushed to below the detection limit. Instead one observes for both ions a small contribution with a peak maximum at 4.4 eV (Cl^-) and 4.6 eV (F^-). The most striking feature, however, is strong desorption from a resonance feature with a nearly identical peak position for both compounds (9.7 eV). From the gas phase species only very weak contributions appear near that energy.

While the complete suppression of the low energy Cl^- and F^- feature can simply be explained by effective energy randomization in the TNI and the kinetic energy filter for desorption, which pushes the desorption signal to below the detection limit, the strong desorption resonance at higher energy is remarkable. It should be noted that this kind of behaviour has been observed before in other systems [17,25]. A particular strong effect was recently reported [34] in the case of CF_3I where a surprisingly intense desorption signal of the four atomic fragment CF_3^- was observed. By comparing the projected density (number of molecules per area) in the gas phase reaction volume with that on the surface it was shown that the absolute number of the desorption cross section exceeds that of the gas phase DA cross section by at least 2 orders of magnitude. Note that this refers to desorption of an ionic fragment and not simply to an enhancement of the DA cross section for an adsorbed molecule. If we use the same estimation we must conclude that the Cl^- desorption cross section near 9.7 eV is also about 2 orders of magnitude higher than the Cl^- gas phase DA cross section. It must be emphasized that not every DA process at the surface leads to desorption of the ionic fragment so that the DA cross section of a CHF_2Cl molecule near 9.7 eV is expected to be enhanced by distinctly more than 2 orders of magnitude.

Such a cross section enhancement can be due to the increased lifetime of a TNI when coupled to an environment. This can occur for ground state (single particle) resonances but in particular in the case of core excited resonances (as in the present one near 9.7 eV). If in the gas phase it is an open channel resonance primarily decaying via electron emission into the associated excited neutral state, solvation may convert it into a longer lived (closed channel) Feshbach resonance thereby suppressing the decay via autodetachment in favour of DA. This will result in an enhancement of the DA cross section at the surface. In the present case of the 9.7 eV resonance one expects Rydberg states as associated neutral states.

Such a development should be gradually observable in clusters of increasing size. Under our expansion conditions (stagnation pressure up to 2 bar) we in fact observe a threshold for Cl^- formation at 8 eV. Toward higher energy this signal is superimposed by a strong background (starting at 11.5 eV) which prevents a detailed study of ion formation in this energy region. This background signal is due to formation of metastable Ar* ($^3P_2$, $^3P_0$) atoms produced via electron impact to the seed gas. These neutral species live long enough and carry sufficient energy to cause a signal when striking the electron multiplier. We are currently preparing experiments using He as seed gas to study negative ion formation from CHF_2Cl clusters in the energy region around 10 eV.

Acknowledgements

Work supported by the Deutsche Forschungsgemeinschaft (Sfb 337, Il 16/15-1, Il 16/16-1) and the Fonds der Chemischen Industrie.

References

[1] L.G. Christorphorou (Ed.), Electron–Molecule Interactions and Their Applications, Vol. I, Academic, Orlando, FL, 1984.
[2] A. Chutjian, A. Garscadden, J.M. Wadehra, Phys. Rep. 264 (1996) 393.
[3] T. Oster, A. Kühn, E. Illenberger, Int. J. Mass Spectrom. Ion Processes 89 (1989) 1.
[4] E. Illenberger, J. Momigny, Gaseous Molecular Ions. An Introduction to Elementary Processes Induced by Ionization, Steinkopff Verlag, Darmstadt/Springer-Verlag, New York, 1992.
[5] H.S.W. Massey, Negative Ions, Cambridge University Press, Cambridge, 1976.
[6] L.G. Christophorou, D.L. McCorkle, A.A. Christodoulides, Electron Attachment Processes, L.G. Christorphorou (Ed.), Vol. I, Academic, Orlando, FL, 1984.
[7] D.R. Lide (Ed.), Handbook of Chemistry and Physics, 78th ed., CRC, Boca Raton, FL, 1997.
[8] F. Weik, E. Illenberger, J. Chem. Phys. 103 (1995) 1406.
[9] S.R. Hunter, L.G. Christophorou, J. Chem. Phys. 80 (1984) 6150.
[10] H. Hotop, D. Klar, J. Kreil, M.-W. Ruf, A. Schramm, J.M. Weber, The Physics of Electronic and Atomic Collisions, L.J. Dubé, J.B.A. Mitchell, J.W. McConkey, C.E. Brion (Eds.), AIP Press, Woodbury, NY, 1995.
[11] S. Matejcik, A. Kiendler, A. Stamatovic, T.D. Märk, Int. J. Mass Spectrom. Ion Processes 149/150 (1995) 311.
[12] D.M. Pearl, P.D. Burrow, J. Chem. Phys. 104 (1994) 2940.
[13] D.M. Pearl, P.D. Burrow, I. Fabrikant, G.A. Gullup, J. Chem. Phys. 102 (1995) 2737.
[14] E.P. Wigner, Phys. Rev. 73 (1948) 1002.
[15] E. Vogt, G.H. Wannier, Phys. Rev. 95 (1954) 1190.
[16] C.E. Klots, Chem. Phys. Lett. 38 (1976) 61.
[17] O. Ingólfsson, F. Weik, E. Illenberger, Int. J. Mass Spectrom. Ion Processes 155 (1996) 1.
[18] E. Illenberger, Chem. Rev. 92 (1992) 1589.
[19] L. Sanche, IEEE Trans. Electr. Insul. 28 (1993) 789.
[20] A. Stamatovic, G.J. Schulz, Rev. Sci. Instrum. 41 (1970) 423.
[21] A.A. Christodoulides, R. Schumacher, R.W. Schindler, Int. J. Chem. Kinet. 10 (1978) 1215.
[22] F.J. Davis, R.N. Compton, D.R. Nelson, J. Chem. Phys. 59 (1973) 2324.
[23] L.G. Christophorou, Atomic and Molecular Radiation Physics, Wiley-Interscience, London, 1971.
[24] G.K. Jarvis, C.A. Mayhew, L. Singleton, S.M. Spyrou, Int. J. Mass Spectrom. Ion Processes 164 (1997) 207.

[25] P. Tegeder, F. Brüning, E. Illenberger, Chem. Phys. Lett., 310 (1999) 79.

[26] T.D. Märk, Int. J. Mass Spectrom. Ion Processes 107 (1991) 143.

[27] P. Rowntree, L. Parenteau, L. Sanche, J. Chem. Phys. 94 (1991) 8570.

[28] I.T. Iakubov, A.G. Khrapak, Rep. Progr. Phys. 45 (1982) 697.

[29] M. Rosenblit, J. Jortner, Phys. Rev. Lett. 75 (1995) 4079.

[30] A.G. Khrapak, W.F. Schmidt, K.F. Volykhin, Phys. Rev. E 51 (1995) 4804.

[31] M. Meinke, E. Illenberger, J. Phys. Chem. 98 (1994) 6601.

[32] J. St. Dixon-Warren, D.V. Heyd, E.T. Jensen, J.C. Polanyi, J. Chem. Phys. 98 (1993) 5954.

[33] M. Michaud, P. Cloutier, L. Sanche, Phys. Rev. B 48 (1993) 11336.

[34] Y. Le Coat, N.M. Hedhili, R. Azria, M. Tronc, O. Ingólfsson, E. Illenberger, Chem. Phys. Lett. 296 (1998) 208.